This is a repository copy of *Atomic-Resolution Spectrum Imaging of Semiconductor Nanowires*.

White Rose Research Online URL for this paper:
http://eprints.whiterose.ac.uk/125289/

Version: Accepted Version

Article:

Atomic-Resolution Spectrum Imaging of Semiconductor Nanowires

Reza R. Zamani,[*,†] Fredrik S. Hage,[‡] Sebastian Lehmann,[†] Quentin M. Ramasse,[‡] and Kimberly A. Dick[†,¶]

Solid State Physics, Lund University, Box 118, Lund 22100, Sweden, SuperSTEM Laboratory, SciTech Daresbury Campus, Keckwick Ln, Warrington WA4 4AD, U.K., and Centre for Analysis and Synthesis, Lund University, Box 124, Lund 22100, Sweden

E-mail: reza.zamani@ftf.lth.se,reza.r.zamani@gmail.com

Abstract

Over the last decade, III-V heterostructure nanowires have attracted a surge of attention for their application in novel semiconductor devices such as tunneling field-effect transistors (TFETs). The functionality of such devices critically depends on the specific atomic arrangement at the semiconductor heterointerfaces. However, most of the currently available characterization techniques lack sufficient spatial resolution to provide local information on the atomic structure and composition of these interfaces. Atomic-resolution spectrum imaging by means of electron energy-loss spectroscopy (EELS) in the scanning transmission electron microscope (STEM) is a powerful technique with the potential to resolve structure and chemical composition with sub-Å spatial resolution, and to provide localized information about the physical properties of the

---

[*]To whom correspondence should be addressed
[†]Solid State Physics, Lund University
[‡]SuperSTEM Laboratory
[¶]Centre for Synthesis and Analysis, Lund University

material at the atomic scale. Here, we demonstrate the use of atomic-resolution EELS to understand the interface atomic arrangement in three-dimensional heterostructures in semiconductor nanowires. We observed that the radial interfaces of GaSb-InAs heterostructure nanowires are atomically abrupt, while the axial interface in contrast consists of an interfacial region where intermixing of the two compounds occurs over an extended spatial region. The local atomic configuration affects the band alignment at the interface and hence the charge transport properties of devices such as GaSb-InAs nanowire TFETs. STEM-EELS thus represents a very promising technique for understanding nanowire physical properties, such as differing electrical behavior across the radial and axial heterointerfaces of GaSb-InAs nanowires for TFET applications.

Keywords

GaSb - InAs, III-V nanowire, heterointerface, aberration-corrected STEM, atomic-resolution EELS, spectrum imaging

Heterojunctions in semiconductor materials play an increasingly crucial role in a wide variety of semiconductor devices, from lasers[1,2] to photovoltaics[3] to many types of transistors[4–6] where the potential to control the electronic behavior by tuning band alignments opens up a wide range of possible uses. Nanostructures such as semiconductor nanowires have shown particular promise for heterojunction engineering, due to both the increased freedom in material design afforded by their small dimensions (as for example in dislocation-free lateral strain relaxation), and to the dependence of band structures on dimensions (owing to quantum size effects). The behavior of the resulting semiconductor device depends critically on the properties of the heterojunction, which in turn is determined by the local atomic arrangement at the junction. The development of new applications based on nanostructures such as heterostructured semiconductor nanowires thus demands the availability of characterization methods that can determine the atomic arrangement with high precision on a very

2

local, atomically-precise scale.

The realization of the structural and compositional aspects of this paradigm at the atomic level, however, has been a challenge since most of the characterization techniques are not able to provide the necessary information with sufficient spatial resolution. Among currently available methods, scanning probe microscopy (SPM) techniques can reach atomic resolution, but can only provide information on the surface structure. Nanobeam X-ray scattering, atom probe microscopy techniques and secondary ion mass spectroscopy (SIMS) can provide information about the volume; however, their spatial resolution cannot reach the atomic level. In this context, spectrum imaging by means of electron energy-loss spectroscopy (EELS) is known as a powerful method for determination of the atomic structure of such complex materials. Thanks to recent technological advancements, i.e. aberration correction and monochromation in scanning transmission electron microscopy (STEM), it is now possible to obtain sub-0.5-Å-sized electron probes, and hence, the spatial resolution of EELS has increased dramatically down to the atomic scale. Therefore, individual atomic columns and even single atoms can be identified.[7–9] Atomic-resolution EELS was first shown in the pioneer works of Batson[10] and Browning *et al*[11] in 1993, and more than a decade after, it was used by Varela *et al* for chemical identification of atomic columns in $SrTiO_3$ in 2004.[12] Spectrum imaging, however, was first performed in 2007 by Bosman *et al* on $Bi_{0.5}Sr_{0.5}MnO_3$[13] and Kimoto *et al* on $La_{0.8}Ba_{0.2}MnO_3$.[14] Ever since, the technique has been used for the characterization of several layered material, especially oxides with large lattice distances such as $BaTiO_3$,[15–18] and recently on tetrahedrally-coordinated semiconductors such as selenides.[19,20]

The application of atomic-resolution EELS to complex nanostructures is promising, since unlike the bulk materials and thin films studied to date, nanostructures generally do not require complex STEM sample preparation that can damage and change the properties of the heterojunction. The potential to study complex 'as grown' nanostructures is thus a significant advantage. On the other hand, 'as grown' structures are particularly challenging

to characterize for several reasons.

On the one hand, the thickness of the nanowires should comply with the thickness requirements of atomic-resolution EELS. Thicker samples increase multiple scattering and hence the background of the spectra, and decrease the signal-to-noise ratio. On the other hand, small lateral dimensions in nanowires (and in general 1D nanostructures) can lead to less mechanical stability and consequently sample drift. In comparison with layered samples, especially when they stick out from the lacey carbon grids (preferred since carbon background signal is avoided), nanowires are much less stable. They can move or roll on the grid or oscillate during scanning. This can also be the case with nanoparticles, although, nanoparticles have the advantage of being fully-supported by a thin amorphous grid.[21,22] Finally, as-grown nanostructures most often have complex geometry with non-uniform thickness in the direction of interest (electron beam direction), and typically also varying composition along multiple axes, often including the beam direction. Therefore, the suitability of this technique for complex structures such as heterostructure semiconductor nanowires has not yet been fully established.

In this study we demonstrate the application of atomic-resolution EELS to determine local atomic-scale composition of interfaces in GaSb-InAs heterostructure nanowires containing both axial and radial heterojunctions. This material system exhibits a broken type-II band alignment and has proven promising for low-power electronic devices such as tunneling field-effect transistors (TFETs)[23,24] and Esaki tunnel diodes.[25] The properties and performance of this heterostructure system are known to be critically sensitive to the structure of the heterojunction, including its abruptness or atomic intermixing as well as to the specifics of the chemical bonding/polarity at the junction. Although the heterointerfaces in GaSb-InAs nanowires have in principle proven functional in both the axial and radial junctions, full development of any device based on this structure will require detailed characterization of the junction properties as a function of fabrication conditions.

Here we demonstrate that interpretable atomically-resolution compositional information can indeed be obtained on axial and radial heterojunctions in InAs-GaSb nanowires with complex geometry, and, varying thickness and composition in the beam direction. The critical technical parameters include a relatively low electron accelerating voltage (100 kV, which minimizes sample damage in these relatively beam-sensitive materials), an extremely low-drift sample stage (below 0.5 Å in a typical 5 min acquisition time). We determine that for the investigated sample, the vapor-liquid-solid (VLS)-grown axial heterojunction exhibits atomic intermixing on a few-nanometer scale, making it considerably less abrupt than the simultaneously-grown radial heterojunction, which appears to be atomically abrupt. This information is important input for the development of nanowire-based devices, and moreover definitively demonstrates the applicability of this technique for nanostructure heterojunctions in general, including those in beam-sensitive, narrow-bandgap, narrower-lattice-parameter materials.

A schematic of the GaAs-GaSb-InAs heterostructured nanowires is shown in Figure 1a together with an overview image acquired by scanning electron microscopy (SEM, ZEISS Leo Gemini 1560 operated at 15 kV). Nanowires are grown on $\langle 111 \rangle$B-oriented GaAs wafers by metal organic vapor phase epitaxy (MOVPE) in an AIXTRON $3 \times 2''$ close couple showerhead reactor operated at a reactor pressure of 100 mbar and a total hydrogen carrier gas flow of 8 standard liters per minute (slm). Growth is performed following the VLS growth mechanism using size-selected Au aerosol particles[26] with a nominal diameter of 18 nm as a catalyst material. After an annealing step in an H_2/AsH_3 atmosphere for 7 minutes at a set temperature of 630°C the GaSb-InAs nanowires are grown on GaAs stems (grown at a set temperature of 510°C) since the growth of Au-seeded antimonide nanowires suffers from nucleation issues.[27,28] When the GaSb nanowire is next grown (also at 510°C), it covers a small segment of GaAs stem, and the diameter increases. Finally, InAs growth is performed at a set temperature of 450°C with the InAs deposited on GaSb in two ways: (i) as an axial segment on top of the GaSb nanowire through VLS growth, and (ii) as a thin InAs shell that covers

the nanowire radially via vapor-solid (VS) growth. The total thickness of the GaSb-InAs core-shell segment is below 40 nm. Trimethylgallium (TMGa), trimethylindium (TMIn), arsine (AsH$_3$), and trimethylantimony (TMSb) were used as precursor materials for Ga, In, As, and Sb respectively. A detailed flow chart for the growth of the GaAs/GaSb/InAs heterostructured nanowires is given in Figure 1b with the corresponding molar fractions (χ) being $\chi_{\mathrm{TMGa}} = 1.3 \times 10^{-5}$ and $\chi_{\mathrm{AsH_3}} = 5.6 \times 10^{-4}$, respectively for the GaAs stem growth, $\chi_{\mathrm{TMGa}} = 8.9 \times 10^{-6}/6.4 \times 10^{-4}$ and $\chi_{\mathrm{TMSb}} = 4.7 \times 10^{-5}/2.3 \times 10^{-5}$, respectively for the GaSb nucleation and growth, and $\chi_{\mathrm{TMIn}} = 1.9 \times 10^{-6}$ and $\chi_{\mathrm{AsH_3}} = 4.8 \times 10^{-4}$, respectively for the InAs growth.

EELS maps and high angle annular dark field (HAADF) STEM images were collected on two dedicated STEM Nion microscopes operating at 100 kV, hereafter denoted US100 and US100MC. The former is a Nion UltraSTEM100, equipped with a third generation Nion probe corrector, a Gatan UHV Enfina EELS spectrometer, and operated here at 100 kV acceleration voltage. The latter is a Nion UltraSTEM 100MC 'HERMES', equipped with a newly-developed C$_5$ Nion probe corrector (full correction up to 6-fold astigmatism C$_{5,6}$) and a UHV Gatan Enfinium ERS spectrometer optimized for high energy resolution with high-stability electronics.[29] Such mid-range voltage is used to minimize beam knock-on damage while retaining very high spatial resolution, 0.78 Å demonstrated at 100 kV, thus perfectly suited to the diamond-like structure of these III-V nanowires). Also ultra-high vacuum (UHV) system is utilized to avoid specimen contamination. Additionally, the specimens are baked prior to the insertion. On the other hand, remarkable environmental conditions are considered in order to provide ideal conditions (magnetic fields, sound, and temperature control) for lengthy analytical experiments without suffering from drift.

EEL spectrum image datasets were dark-subtracted and then de-noised using Principal Component Analysis (PCA) as implemented in the MSA plugin for Gatan's Digital Micrograph software (commercially available from HREM Research Inc.).[30] EELS maps are generated by (i) subtracting the decaying background using a power law, by taking a typical

50-70 eV window before the $M_{4,5}$ edges of In (443 eV) and Sb (528 eV), and L_3 of Ga (1115 eV) and As (1323 eV), then (ii) extracting the signal by placing a 50- to 70-eV-wide window starting at the mentioned edges. 3D atomic models were created by using the Rhodius software package.[31]

Before moving on to the atomic structure of the heterointerfaces, we describe the entire material system in order to clarify the morphology. In Figure 2 we show the overview EELS maps of the axial and radial interfaces of a GaAs-GaSb-InAs heterostructure nanowire, revealing the transition from GaAs to GaSb and then to InAs. The EELS maps taken from the lower part of the nanowire (Figure 2i-o) reveal how GaSb and InAs cover the GaAs stem. Apparently, while the GaSb grows axially on the GaAs stem, it also covers a part of the stem at a much slower rate. This down-growth follows a three-fold symmetry as can be seen in the EELS maps confirmed by the HAADF-STEM intensity profiles shown in the Supporting Information (SI) in Figure SI1. Afterwards, InAs also covers a part of the stem in the same fashion. This three-fold symmetry can be related to the surface polarity (polarity is the internal electric field of the crystal caused by the asymmetry in the charge distribution of a cation-anion bond in tetrahedrally coordinated compound semiconductors such as III-V and II-VI.[32] The terminating element at the surface determines the surface polarity). The GaAs stem forms side facets from the {112} family which are semi-polar planes: three of them are A-polar while the other three are B-polar. According to the polarity analysis shown in Figure SI2, Ga-polar surfaces show a higher degree of overgrowth. This is in good agreement with the higher surface energy of Ga-polar surfaces in comparison with the As-polar ones.[33] The InAs radial overgrowth on the GaSb segment does not show such three-fold symmetry. A similar InAs thickness on both sides of the nanowire instead indicates rather similar growth rates on all facets. This is reasonable since VLS-grown GaSb under these conditions typically exhibits {110} facets,[34] which are non-polar.

The upper axial/radial interface between GaSb and InAs is shown in Figure 2b-h. The EELS maps reveal that the axial interface is not a flat $(\bar{1}\bar{1}\bar{1})$ surface. This also suggests a

three-fold symmetry along the nanowire growth axis, similar to the InAs neck of the nanowire below the Au droplet. The outer morphology of the top part (neck) of the nanowire (outer InAs surface) indicates three {111} and three {100} facets. The inner morphology (GaSb-InAs axial interface), according to the EELS maps, is consistent with three {122} and three {311} facets in the same three-fold-symmetry fashion as the lower part mentioned above.

In the overview maps both the radial and axial interfaces seem to show abrupt compositional transitions. This is consistent with previous energy-dispersive X-ray spectroscopy (EDX) analysis on similar structures, which indicated interfaces apparently sharp within an estimated resolution limit of about 3 nm.[34] As mentioned above, such overview maps as given in Figure 2 provide information about the inner morphology and the facets at the heterointerfaces. However, for more detailed information about the quality and composition of the heterointerfaces, we need to resolve the structures at the atomic scale. Therefore, in the following we focus on atomic-resolution EELS mapping of such interfaces.

Figure 3a shows an overview HAADF-STEM image of the GaSb-InAs radial heterostructure, with a high-resolution close-up view of the radial heterojunction section indicated by the white box shown in Figure 3b. Atomic-resolution EELS maps of the interfacial region indicated in Figure 3b are displayed in Figure 3c-i. They reveal an abrupt transition from GaSb to InAs at the position of the heterojunction. By overlaying each pair of elemental maps we create composite color images of Ga-Sb (Figure 3c,e), and In-As (Figure 3d,f). In these composite maps we clearly visualize the III-V dumbbell units (Figure 3g and Figure 3h, showing Ga-Sb and In-As dumbbells, respectively) revealing the B-polarity in the growth direction and A-polarity in this particular radial direction. This conclusion is consistent with a visual inspection of atomic-resolution HAADF-STEM images, in which the heavier element in the dumbbell pair is expected to appear brighter (Figure 3b). By overlaying the EELS maps of all four elements (Figure 3i) we determine that at the interface there is only one atomic bilayer in which the signals of all four elements are detected. This is attributed to the 3D morphology of the investigated core-shell structure. As the side facets

of the nanowire are of the {110} plane family (Figure SI2), the InAs-GaSb interface imaged from [01$\bar{1}$] zone axis (ZA) is in fact a corner where the two {110}-type facets meet (the side facets are not parallel to the viewing direction). Moreover, the shell covers the entire core structure. Therefore, in the region close to the interface the core is rather thin and in size comparable with the shell, which makes this atomic bilayer appear as a mix of the two compounds. In addition, weak signals of In and As can also be detected from the region of GaSb core farther from the border. They originate from the InAs shell covering the entire structure. This is in contrast to the InAs part where no Ga or Sb signal can be detected since only the InAs shell is probed. In Figure 3j-m we show the extracted EELS signals of the four elements from the regions indicated by 3x3 pixel squares. Note that a minimum signal of In and Sb can be detected away from these atoms which is due to the delocalization effect of the EELS signals.[35] Being aligned to a specific zone axis also adds complexity in that the propagation of the beam and associated channeling effects would need to be considered to fully quantify the resulting maps. In addition, delocalization affects low energy edges more strongly, and is therefore expected to be more pronounced for Sb and In than for Ga and As in the present material system. The intensity scales are shown in Figure 3 beside the EELS maps. The minimum Ga signal detected at the right side of the map, the furthest point from the heterointerface and the core, in only 2% of the maximum counts. For Sb this minimum increases to 13%. In the case of In and As, the minimum counts, detected from the left side of the map, are much higher (18% for As and 22% for In), as the thin InAs shell around the core still contributes to the recorded signal. Due to complex beam propagation and dynamical effect, the precise (and indeed quantitative) interpretation of atomically-resolved EELS data would normally require a careful comparison to inelastic image simulations[36] or the use of a recently proposed inversion procedure.[37] Beam channeling could in particular account for the observed diffuse nature of the axial interface, at least in part and we are exploring the use of these numerical techniques to provide further insight into the precise structure of the heterointerfaces in this system. Nevertheless, our results still highlight clear differences,

9

within the same nanowire and in otherwise identical condition, between the diffuse axial interfaces which retain the cation dumbbell polarity and the sharp radial interfaces for which we demonstrated a striking compound transition.

After the thorough study of the radial heterointerface between GaSb and InAs, we now move to the discussion of the axial interfaces. Atomic-resolution EELS analysis of the axial heterojunction is shown in Figure 4. In contrast to the radial heterointerface, intermixing of the two compounds occurs along the axial direction, despite this interface appearing sharp at lower resolution spectrum imaging shown in Figure 2. A part of the axial interface is shown in the high-resolution HAADF image in Figure 4b, with the interfaces (as determined in Figure 2) indicated by dashed lines as a guide to the eye. Figure 4c-h show the EELS maps obtained from the axial GaSb-InAs heterointerface, from the region indicated by the white rectangle in Figure 4b. Note that the data presented here were systematically recorded near the lateral facet where the nanowire becomes thinner, in order to provide a better clarity and reliability of the extracted chemical maps. At this interface, some atomically-localized Ga and Sb signals can be seen in the EEL spectra above the interface between the GaSb and InAs, suggesting some strong intermixing of the two compounds at the beginning of InAs segment. A gradual decay of Ga and Sb signals towards the top can be seen in Figure 4c and e, respectively. We attribute this to the residual Ga and Sb atoms present in the Au droplet during the VLS growth of the InAs segment. Although residual Sb in the InAs segment is consistent with previous reports, the intermixing of Ga/In occurs only in the first few atomic layers and was thus beyond the resolution limit of previous investigations.[34] Nevertheless, this intermixing in the first layers has significant implications for the band structure and properties of the heterojunction.

Another point to take into account is the relatively strong signal of As in the GaSb region. This signal partially originates from the InAs shell that is covering the entire GaSb segment. However, towards the bottom of the investigated segment the In signal decays faster. This suggests the possible interdiffusion of the group V element, where some As diffuses backwards

10

into the grown GaSb segment. Although the As signal is strong in the first few nanometers below the axial heterointerface, it decreases considerably just below this interfacial area as shown in the atomic-resolution EELS maps in Figure SI3. In comparison with the EELS maps in Figure 3, the signal count minima of the elements are much lower as indicated in the corresponding intensity scales. This is due to the fact that the investigated area (the EELS maps) in Figure 4 extends further away from the axial interface and thus EELS signal delocalization does not play a role. Therefore, the minima of In and As signals (8% and 13% of the maxima, respectively) detected from the bottom-most part of the map, is due to the actual presence of the elements. Moreover, it is worth noting that these elemental signals are highly localized to the atomic columns. Therefore, even with delocalization playing a role, significant amount of the elemental signals are detected from the corresponding atomic columns (both Ga and In from group III atomic columns, and Sb and As from group V atomic columns). The EELS signals of the four elements from the indicated regions are shown in Figure 4i-l.

Although the axial and radial heterojunctions are formed simultaneously in the growth reactor, the analysis carried out here indicates that they differ significantly at the atomic scale. There are several reasons for this. The group III intermixing can most likely be attributed to a 'reservoir effect' in the Au droplet, where residual Ga and Sb atoms are retained slightly past the point of switching. This effect is known to cause intermixing and significant interfacial grading in many semiconductor heterostructures, including Si-Ge,[38] InAs-InP,[39] InAs-GaAs,[40] and GaAs-GaP nanowires.[41] Previous investigations have consistently found the Ga-In switch to be significantly sharper than the corresponding In-Ga switch,[42,43] but here we demonstrate that some very local intermixing occurs in the former case as well. The apparent interchange of group V elements (indicated by the decreasing As signal downwards from the apparent heterojunction) most probably has a different origin. The different growth directions of the axial and radial structures might be critical in this case, with the axial polar direction exhibiting significantly more interdiffusion.

The results discussed here demonstrate the need for very high spatial resolution and local compositional information to understand the heterjunctions in complex nanostructures. In fact, atomic-resolution EEL spectrum imaging is the only available technique that can provide atomically-resolved information about the chemical signatures at the heterointerfaces of such structures with complex 3D geometry. It should be noted that recent technical developments have made chemical mapping using energy-dispersive X-ray spectroscopy (EDX) possible at atomic resolution.[44,45] For relatively heavy elements such as those present in our system, and for which X-ray spectroscopy is traditionally considered favorable, this technique would have also been perfectly suited. As with EELS, however, very few real-life example applications on III-V systems have been reported,[46] as the technique is getting more widely used and its advantages and limitations are being investigated. Arguably, and in spite of the much higher count rates provided in particular with multi-detector geometries, very high beam currents are typically recommended for EDX mapping within timeframes comparable with EELS experiments, which in some cases can be detrimental and lead to sample damage.

In summary, we use atomic-resolution aberration-corrected STEM/EELS spectrum imaging to obtain crucial experimental spectroscopic information about the chemical and structural aspects of the heterointerfaces in a complex GaSb-InAs nanostructure of interest for low-power electronics applications. Although the material system is challenging for mapping, we can maximize information content, by paying great attention to using appropriate experimental conditions (minimizing knock-on damage, contamination, and drift). We demonstrate, for the example system of GaSb-InAs axial/radial heterostructure nanowires, that the interfaces along different axes in the same nanostructure can be analyzed and compared.

In this case, we observe that the radial heterointerface is atomically sharp, while the axial interface, which is not optimized, exhibits intermixing and complex composition especially in the first atomic layers. The abruptness of the radial interface and the intermixing of the axial one have important implications for the band structure and for understanding the electronic behavior of the junctions. This method, in addition, opens up the possibility

of direct measurement of the electronic band structure at the atomic scale by means of monochromated low-loss EELS mapping.[47] It has the potential to reveal the differences of the band gap alignment across the axial and radial heterointerfaces. Moreover, by improving the tilting features, one can attempt discrete tomography EEL spectrum imaging approaches in order to reconstruct the 3D heterointerfaces at the atomic scale, although detailed inelastic images simulations would be necessary to reach a faithful reconstruction - which may be computationally prohibitive in all but a few cases.

The information provided by this method can facilitate the precise study and understanding of the growth mechanisms, through which we can obtain full control over the chemical composition of the heterostructured systems. Moreover, detailed analysis should in principle allow us to couple these growth mechanisms to resulting electronic properties. The results shown here indicate the methods are applicable not only to this specific material system, but to a wide variety of nanostructures with varying geometry and composition along multiple axes.

Acknowledgement

References

(1) Ho, J.; Tatebayashi, J.; Sergent, S.; Fong, C. F.; Iwamoto, S.; Arakawa, Y. *ACS Photonics* **2015**, *2*, 165–171.

(2) Saxena, D.; Jiang, N.; Yuan, X.; Mokkapati, S.; Guo, Y.; Tan, H. H.; Jagadish, C. *Nano Letters* **2016**, *16*, 5080–5086, PMID: 27459233.

(3) Czaban, J. A.; Thompson, D. A.; LaPierre, R. R. *Nano Letters* **2009**, *9*, 148–154, PMID: 19143502.

(4) Lind, E.; Persson, A. I.; Samuelson, L.; Wernersson, L.-E. *Nano Letters* **2006**, *6*, 1842–1846, PMID: 16967988.

(5) Nilsson, H. A.; Duty, T.; Abay, S.; Wilson, C.; Wagner, J. B.; Thelander, C.; Delsing, P.; Samuelson, L. *Nano Letters* **2008**, *8*, 872–875, PMID: 18302328.

(6) Dhungana, K. B.; Jaishi, M.; Pati, R. *Nano Letters* **2016**, *16*, 3995–4000, PMID: 27280769.

(7) Geaney, H.; Mullane, E.; Ramasse, Q. M.; Ryan, K. M. *Nano Letters* **2013**, *13*, 1675–1680, PMID: 23517564.

(8) Senga, R.; Komsa, H.-P.; Liu, Z.; Hirose-Takai, K.; Krasheninnikov, A. V.; Suenaga, K. *Nature Materials* **2014**, *13*, 1050–1054.

(9) Tizei, L. H.; Iizumi, Y.; Okazaki, T.; Nakanishi, R.; Kitaura, R.; Shinohara, H.; Suenaga, K. *Ultramicroscopy* **2016**, *160*, 239 – 246.

(10) Batson, P. E. *Nature* **1993**, *366*, 727–728.

(11) Browning, N. D.; Chisholm, M. F.; Pennycook, S. J. *Nature* **1993**, *366*, 143–146.

(12) Varela, M.; Findlay, S. D.; Lupini, A. R.; Christen, H. M.; Borisevich, A. Y.; Dellby, N.; Krivanek, O. L.; Nellist, P. D.; Oxley, M. P.; Allen, L. J.; Pennycook, S. J. *Physical Review Letters* **2004**, *92*.

(13) Bosman, M.; Keast, V. J.; García-Muñoz, J. L.; D'Alfonso, A. J.; Findlay, S. D.; Allen, L. J. *Phys. Rev. Lett.* **2007**, *99*, 086102.

(14) Kimoto, K.; Asaka, T.; Nagai, T.; Saito, M.; Matsui, Y.; Ishizuka, K. *Nature* **2007**, *450*, 702–704.

(15) Muller, D. A.; Kourkoutis, L. F.; Murfitt, M.; Song, J. H.; Hwang, H. Y.; Silcox, J.; Dellby, N.; Krivanek, O. L. *Science* **2008**, *319*, 1073–1076.

(16) Botton, G. A.; Lazar, S.; Dwyer, C. *Ultramicroscopy* **2010**, *110*, 926–934.

(17) Kociak, M.; Stéphan, O.; Walls, M. G.; Tencé, M.; Colliex, C. In *Scanning Transmission Electron Microscopy: Imaging and Analysis*; Pennycook, S. J., Nellist, P. D., Eds.; Springer New York: New York, NY, 2011; pp 163–205.

(18) Varela, M.; Gazquez, J.; Pennycook, S. J. *MRS Bulletin* **2012**, *37*, 29–35.

(19) Sanli, E. S.; Ramasse, Q. M.; Sigle, W.; Abou-Ras, D.; Mainz, R.; Weber, A.; Kleebe, H.-J.; van Aken, P. A. *Journal of Applied Physics* **2016**, *120*, 205301.

(20) Sanli, E. S.; Ramasse, Q. M.; Mainz, R.; Weber, A.; Abou-Ras, D.; Sigle, W.; van Aken, P. A. *Applied Physics Letters* **2017**, *111*, 032103.

(21) Xin, H. L.; Mundy, J. A.; Liu, Z.; Cabezas, R.; Hovden, R.; Kourkoutis, L. F.; Zhang, J.; Subramanian, N. P.; Makharia, R.; Wagner, F. T.; Muller, D. A. *Nano Letters* **2012**, *12*, 490–497.

(22) Zhu, Y.; Ramasse, Q. M.; Brorson, M.; Moses, P. G.; Hansen, L. P.; Kisielowski, C. F.; Helveg, S. *Angewandte Chemie International Edition* **2014**, *53*, 10723–10727.

(23) Borg, B. M.; Dick, K. A.; Ganjipour, B.; Pistol, M.-E.; Wernersson, L.-E.; Thelander, C. *Nano Letters* **2010**, *10*, 4080–4085.

(24) Dey, A. W.; Borg, B. M.; Ganjipour, B.; Ek, M.; Dick, K. A.; Lind, E.; Thelander, C.; Wernersson, L.-E. *IEEE Electron Device Letters* **2013**, *34*, 211–213.

(25) Ganjipour, B.; Dey, A. W.; Borg, B. M.; Ek, M.; Pistol, M.-E.; Dick, K. A.; Wernersson, L.-E.; Thelander, C. *Nano Letters* **2011**, *11*, 4222–4226.

(26) Magnusson, M. H.; Deppert, K.; Malm, J.-O.; Bovin, J.-O.; Samuelson, L. *Nanostructured Materials* **1999**, *12*, 45 – 48.

(27) Borg, B. M.; Wernersson, L.-E. *Nanotechnology* **2013**, *24*, 202001.

(28) Tornberg, M.; Martensson, E.; Zamani, R. R.; Lehmann, S.; Dick, K. A.; Gorji Ghalamestani, S. *Nanotechnology* **2016**, *27*, 175602.

(29) Ramasse, Q. M. *Ultramicroscopy* **2017**, *180*, 41 – 51, Ondrej Krivanek: A research life in EELS and aberration corrected STEM.

(30) https://www.hremresearch.com/Eng/plugin/MSAEng.html,

(31) Bernal, S.; Botana, F. J.; Calvino, J. J.; López-Cartes, C.; Pérez-Omil, J. A.; Rodríguez-Izquierdo, J. M. *Ultramicroscopy* **1998**, *72*, 135–164.

(32) Zamani, R. R.; Gorji Ghalamestani, S.; Niu, J.; Skold, N.; Dick, K. A. *Nanoscale* **2017**, *9*, 3159–3168.

(33) Moll, N.; Kley, A.; Pehlke, E.; Scheffler, M. *Phys. Rev. B* **1996**, *54*, 8844–8855.

(34) Ek, M.; Borg, B. M.; Dey, A. W.; Ganjipour, B.; Thelander, C.; Wernersson, L.-E.; Dick, K. A. *Crystal Growth & Design* **2011**, *11*, 4588–4593.

(35) Egerton, R. F. *Springer, New York* **1986**, *226*.

16

(36) Neish, M. J.; Oxley, M. P.; Guo, J.; Sales, B. C.; Allen, L. J.; Chisholm, M. F. *Physical Review Letters* **2015**, *114*.

(37) Forbes, B. D.; D'Alfonso, A. J.; Williams, R. E. A.; Srinivasan, R.; Fraser, H. L.; McComb, D. W.; Freitag, B.; Klenov, D. O.; Allen, L. J. *Physical Review B* **2012**, *86*.

(38) Wu, Y.; Fan, R.; Yang, P. *Nano Letters* **2002**, *2*, 83–86.

(39) Björk, M. T.; Ohlsson, B. J.; Sass, T.; Persson, A. I.; Thelander, C.; Magnusson, M. H.; Deppert, K.; Wallenberg, L. R.; Samuelson, L. *Nano Letters* **2002**, *2*, 87–89.

(40) Dick, K. A.; Bolinsson, J.; Borg, B. M.; Johansson, J. *Nano Letters* **2012**, *12*, 3200–3206, PMID: 22642741.

(41) Gudiksen, M. S.; Lauhon, L. J.; Wang, J.; Smith, D. C.; Lieber, C. M. *Nature* **2002**, *415*, 617–620.

(42) Paladugu, M.; Zou, J.; Guo, Y.-N.; Zhang, X.; Kim, Y.; Joyce, H. J.; Gao, Q.; Tan, H. H.; Jagadish, C. *Applied Physics Letters* **2008**, *93*, 101911.

(43) Krogstrup, P.; Yamasaki, J.; Sorensen, C. B.; Johnson, E.; Wagner, J. B.; Pennington, R.; Aagesen, M.; Tanaka, N.; Nygard, J. *Nano Letters* **2009**, *9*, 3689–3693, PMID: 19842690.

(44) D'Alfonso, A. J.; Freitag, B.; Klenov, D.; Allen, L. J. *Physical Review B* **2010**, *81*.

(45) Allen, L. J.; D'Alfonso, A. J.; Freitag, B.; Klenov, D. O. *MRS Bulletin* **2012**, *37*, 47–52.

(46) Klenov, D. O.; Zide, J. M. O. *Applied Physics Letters* **2011**, *99*, 141904.

(47) Keller, D.; Buecheler, S.; Reinhard, P.; Pianezzi, F.; Bissig, B.; Carron, R.; Hage, F.; Ramasse, Q.; Erni, R.; Tiwari, A. N. *Applied Physics Letters* **2016**, *109*, 153103.

Atomic-Resolution Spectrum Imaging of Semiconductor Nanowire Devices

Reza R. Zamani, Fredrik S. Hage, Sebastian Lehmann, Quentin M. Ramasse, Kimberly A. Dick

Solid State Physics, Lund University, Box 118, Lund 22100, Sweden

Centre for Analysis and Synthesis, Lund University, Box 124, Lund 22100, Sweden

E-mail: reza.zamani@ftf.lth.se, reza.r.zamani@gmail.com

Morphology

Figure SI1 confirms the three-fold symmetry of the down-grown GaSb/InAs cover on the GaAs stem, as shown in Figure 2 and discussed in the paper. The first intensity profile reveals the symmetric hexagonal cross-section of the GaSb-InAs core-shell structure. The second and third intensity profiles, however, indicate the three-fold symmetry in which the GaSb and InAs cover only three of the lateral facets of the GaAs stem.

Figure SI2 shows that the three covered facets of the GaAs stem are Ga-polar.

EELS maps below the axial heterointerface

Figure SI3 shows EELS maps obtained from the area below the axial GaSb-InAs heterointerface. A few nanometers below this interfacial region, the As signal drops significantly. The In signal already dropped earlier as shown in Figure 4. There is always a minimum amount of energy-loss electrons related to the In and As edges, which are originated from the thin InAs shell around the GaSb core.

This material is available free of charge via the Internet at `http://pubs.acs.org/`.

Graphical TOC Entry
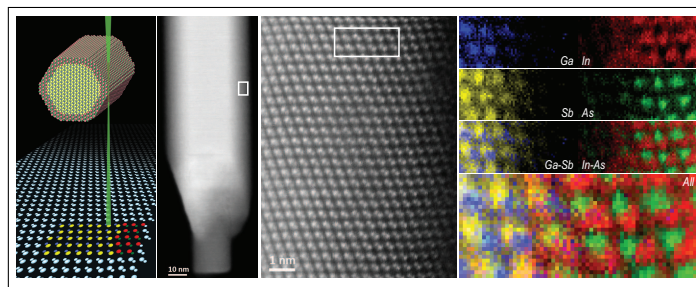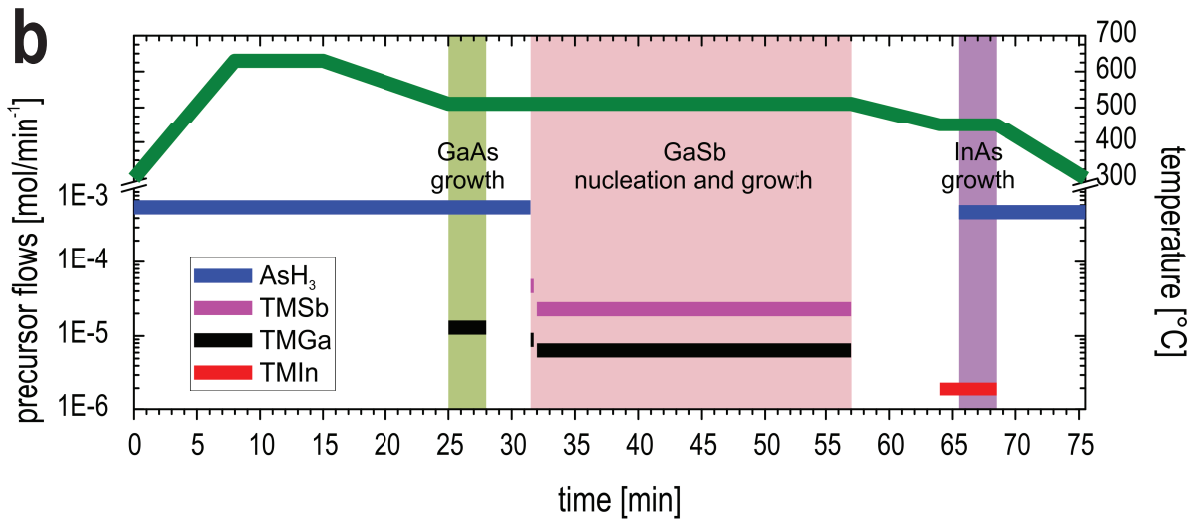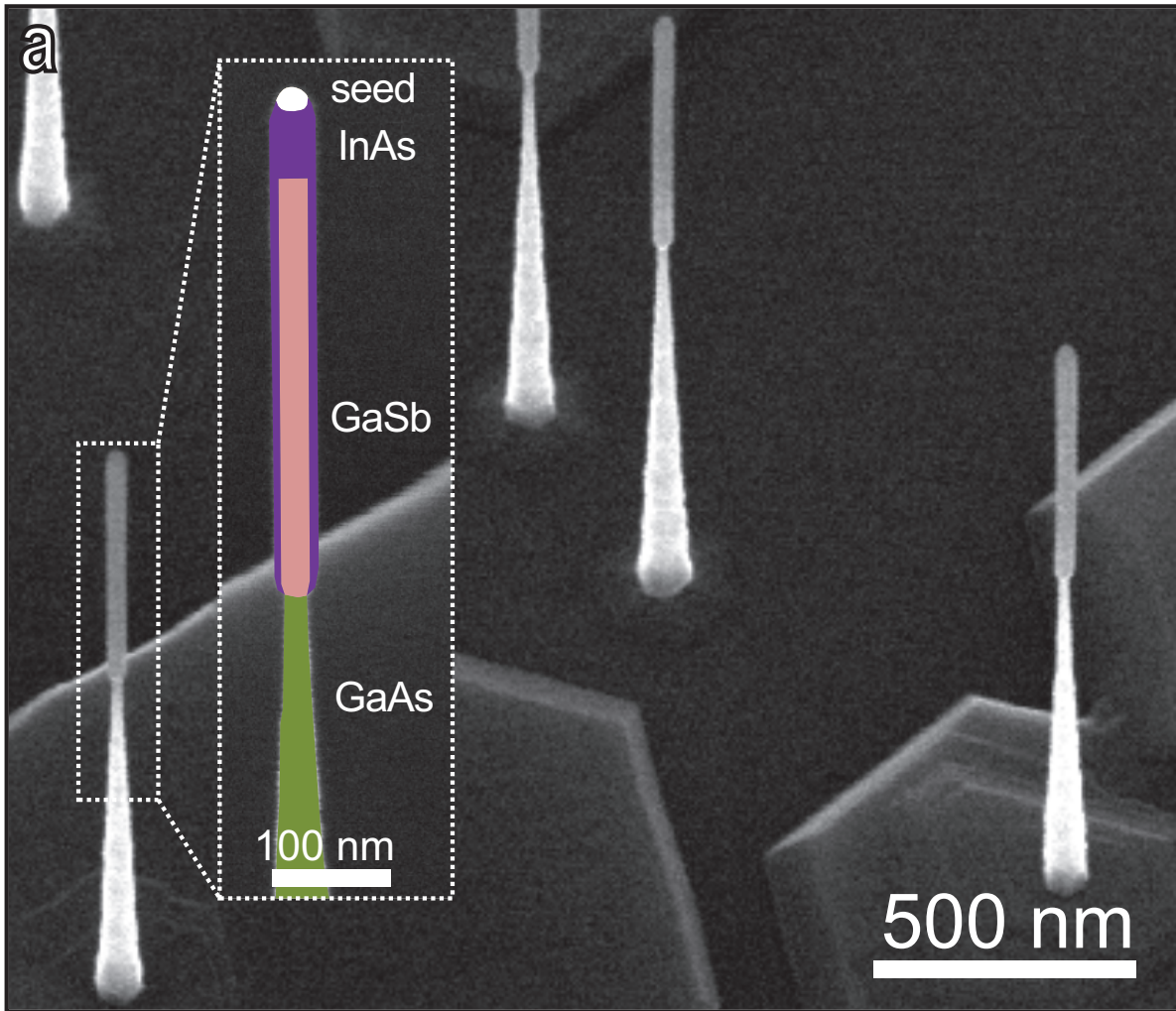
Figure 1: (a) SEM micrograph of GaSb-InAs heterostructure nanowires grown on GaAs stems on a ⟨111⟩B-oriented GaAs wafer, (b) schematics of the precursor molar fractions and temperature of the growth process
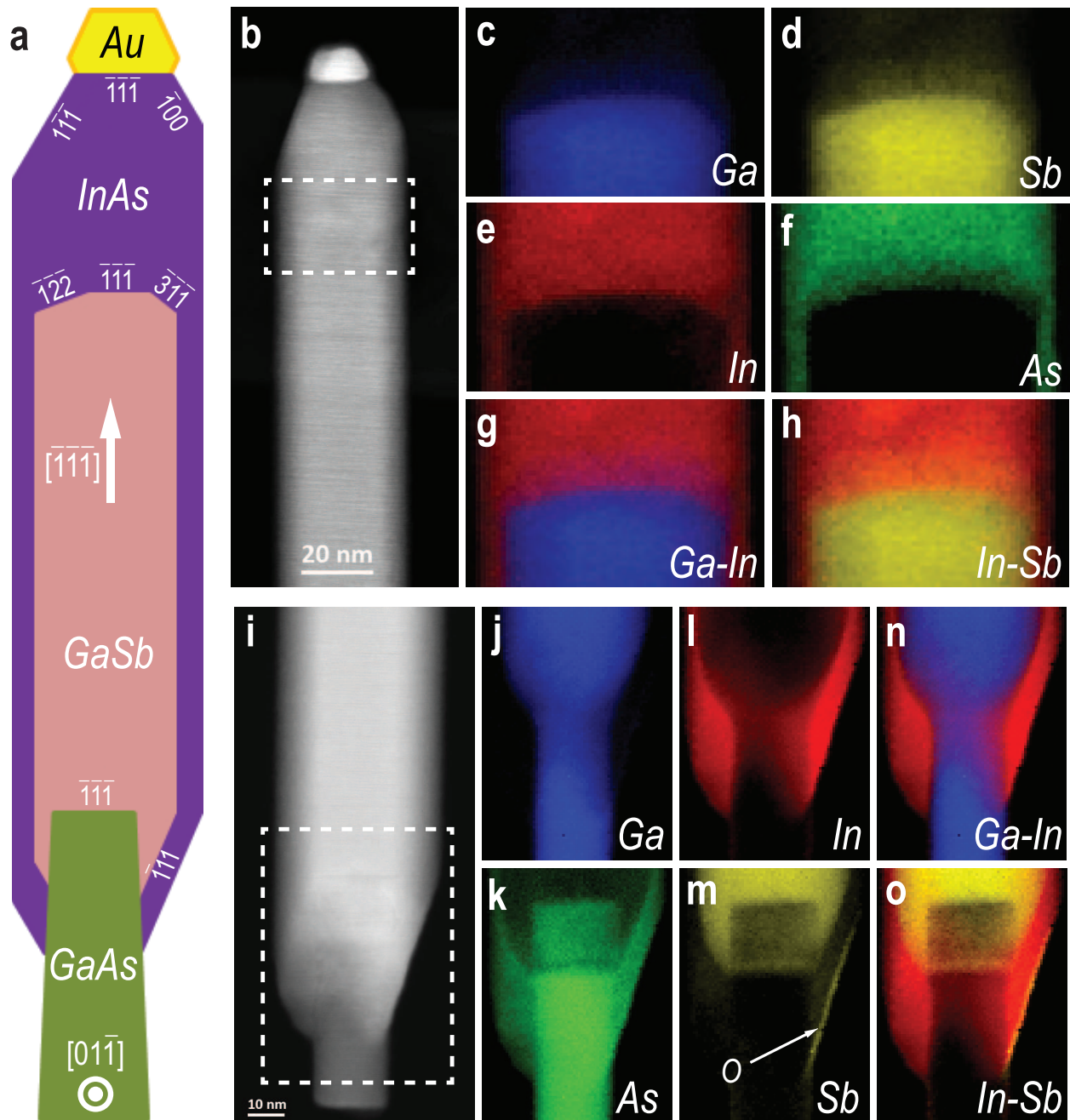
Figure 2: Overview EELS maps of a GaAs-GaSb-InAs heterostructure nanowire (a) schematic illustration of the nanowire showing the inner morphology and the crystallographic facets, (b) HAADF-STEM image of the upper part of the nanowire associated with (c-h) the corresponding EELS maps of the four elements: (c) Ga in blue, (d) Sb in yellow, (e) In in red, (f) As in green, (g) Ga and In, (h) In and Sb; (i) HAADF-STEM image of the upper part of the nanowire associated with (j-o) the corresponding EELS maps of the four elements: (j) Ga in blue, (k) As in green (l) In in red, (m) Sb in yellow, (n) Ga and In, (o) In and Sb.
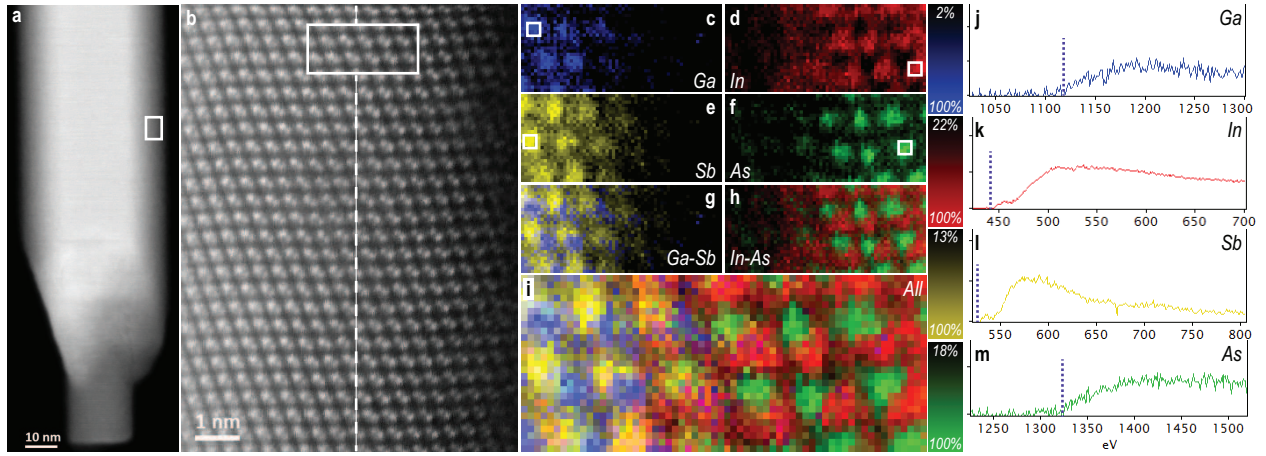
Figure 3: Atomic-resolution EEL spectrum imaging of the GaSb-InAs radial heterointerface (a) low-magnification HAADF-STEM image showing the overview of the nanowire, (b) atomic-resolution HAADF-STEM image of the radial heterointerface revealing the nanowire polarity, (c-i) EELS maps at the radial heterointerface (c) Ga in blue, (d) In in red, (e) Sb in yellow, (f) As in green, (g) Ga and Sb, (h) In and As, and (i) all four elements, (j-m) EELS signals corresponding to the indicated 3x3 pixel squares in (c-f).
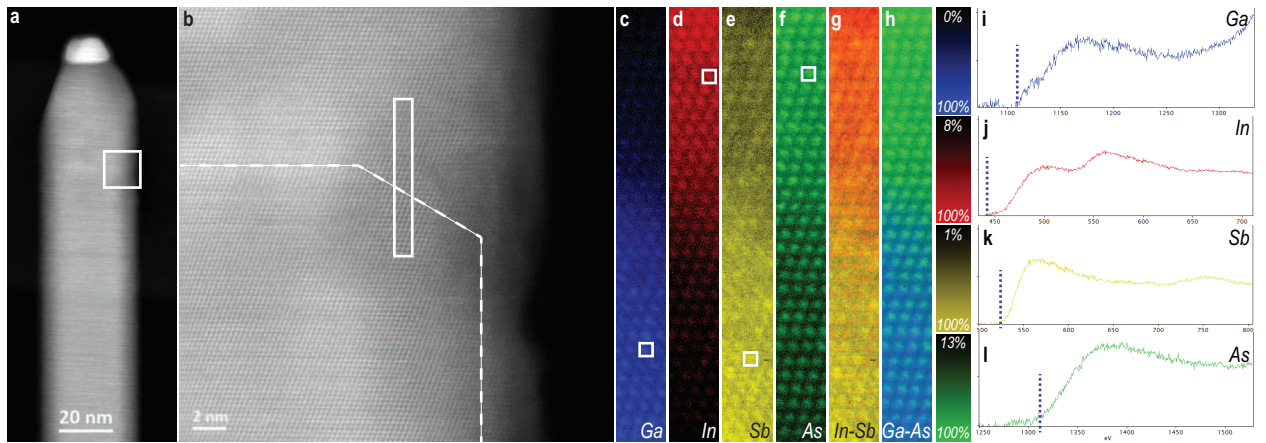

Figure 4: Atomic-resolution EEL spectrum imaging of the GaSb-InAs axial heterointerface (a) low-magnification HAADF-STEM image showing the overview of the nanowire, (b) atomic-resolution HAADF-STEM image of the axial heterointerface, (c-h) EELS maps at the radial heterointerface (c) Ga in blue, (d) In in red, (e) Sb in yellow, (f) As in green, (g) In and Sb, (h) Ga and As, (i-l) EELS signals corresponding to the indicated 12x12 pixel squares in (c-f).

<div align="center">22</div>
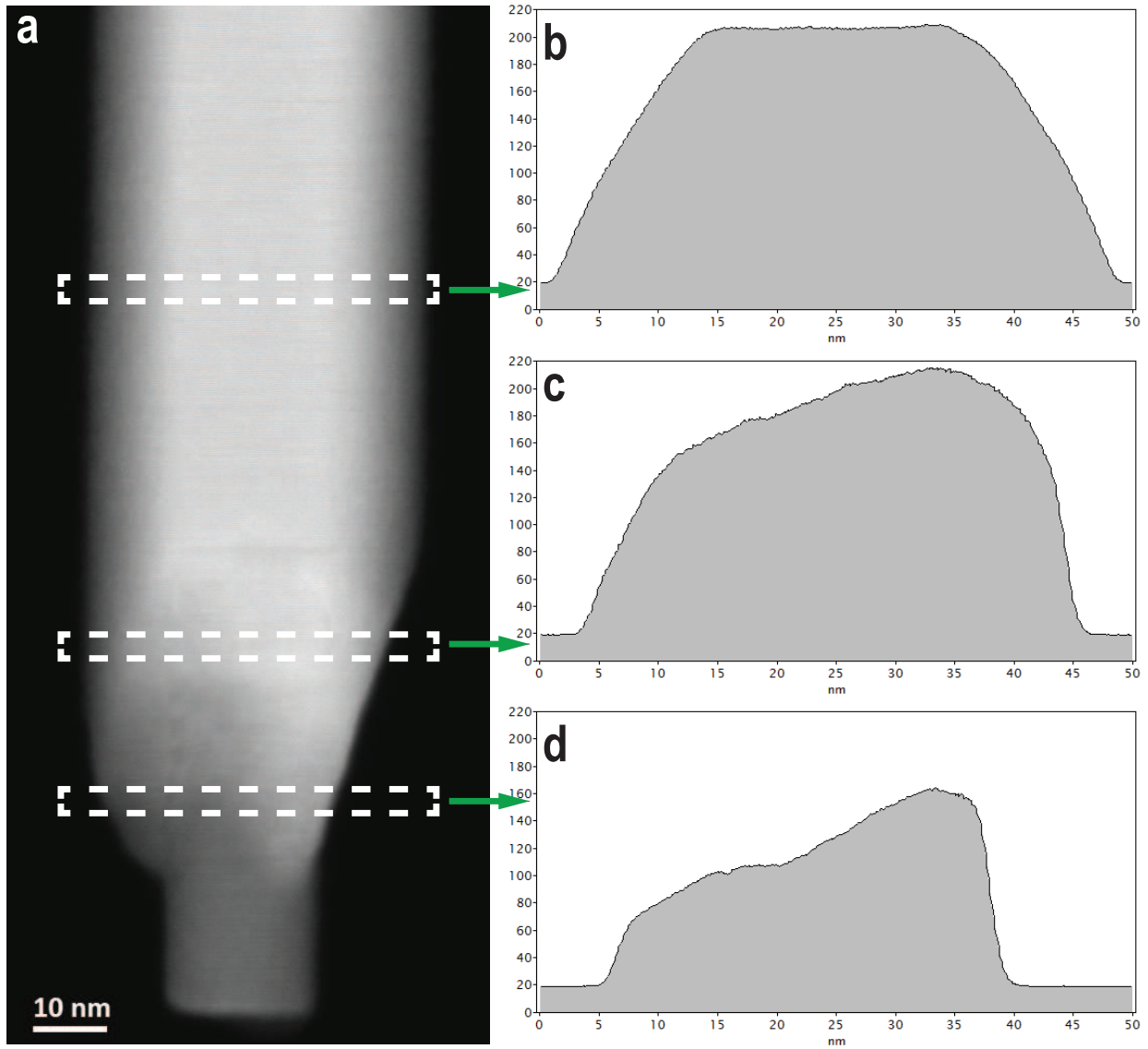
Figure SI1: (a) HAADF-STEM image of a GaAs-GaSb-InAs heterostructure nanowire with (b-d) the corresponding intensity profiles
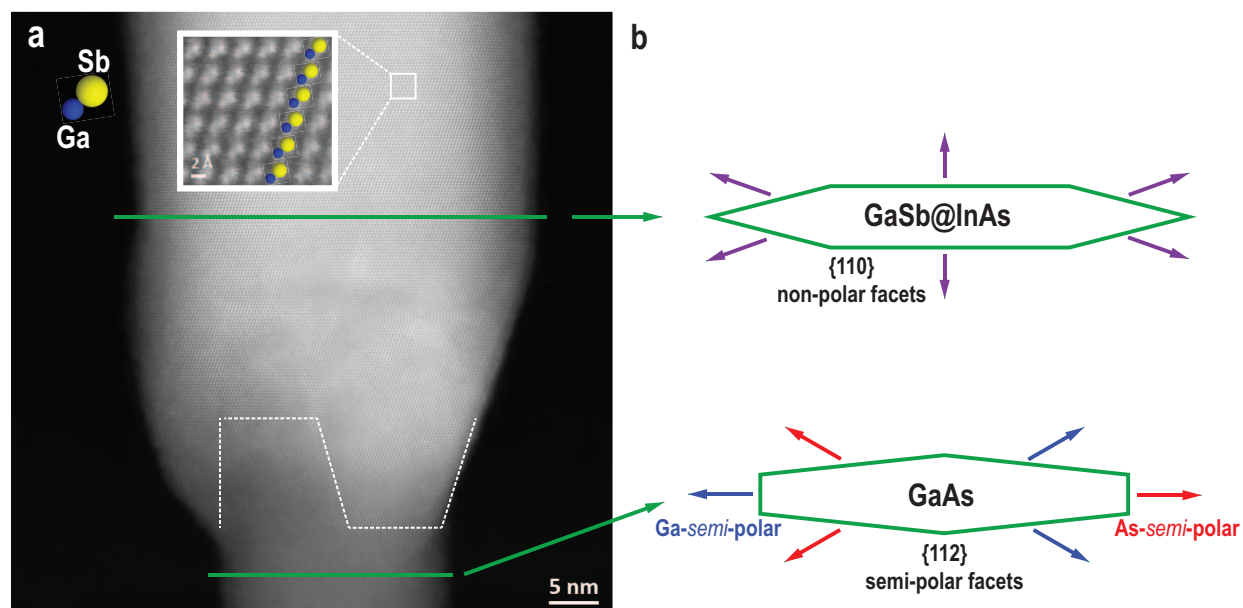
Figure SI2: (a) HAADF-STEM image of a GaAs-GaSb-InAs heterostructure nanowire showing the polarity (inset) and (b) schemes showing the polarity of the lateral facets
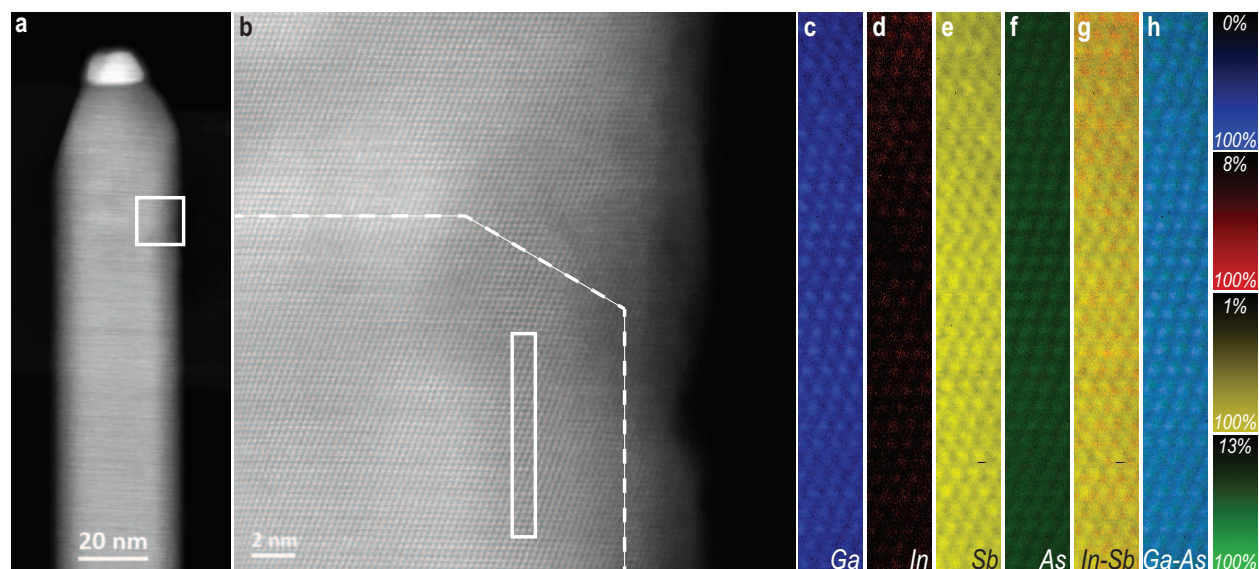

Figure SI3: Atomic-resolution EEL spectrum imaging of the area below the GaSb-InAs axial heterointerface (a) low-magnification HAADF-STEM image showing the overview of the nanowire, (b) atomic-resolution HAADF-STEM image of the axial heterointerface, (c-h) EELS maps at the radial heterointerface (c) Ga in blue, (d) In in red, (e) Sb in yellow, (f) As in green, (g) In and Sb, (h) Ga and As